JGR Atmospheres

Decadal Variabilities in Tropospheric Nitrogen Oxides Over United States, Europe, and China

Zhe Jiang[1] , Rui Zhu[1], Kazuyuki Miyazaki[2] , Brian C. McDonald[3], Zbigniew Klimont[4], Bo Zheng[5], K. Folkert Boersma[6,7], Qiang Zhang[8] , Helen Worden[9] , John R. Worden[2] , Daven K. Henze[10] , Dylan B. A. Jones[11] , Hugo A. C. Denier van der Gon[12] , and Henk Eskes[7]

[1]School of Earth and Space Sciences, University of Science and Technology of China, Hefei, China, [2]Jet Propulsion Laboratory, California Institute of Technology, Pasadena, CA, USA, [3]NOAA Chemical Sciences Laboratory, Boulder, CO, USA, [4]International Institute for Applied Systems Analysis (IIASA), Laxenburg, Austria, [5]Institute of Environment and Ecology, Tsinghua Shenzhen International Graduate School, Tsinghua University, Shenzhen, China, [6]Meteorological and Air Quality department, Wageningen University, Wageningen, The Netherlands, [7]Royal Netherlands Meteorological Institute, De Bilt, The Netherlands, [8]Department of Earth System Science, Ministry of Education Key Laboratory for Earth System Modeling, Tsinghua University, Beijing, China, [9]Atmospheric Chemistry Observations and Modeling Laboratory, National Center for Atmospheric Research, Boulder, CO, USA, [10]Department of Mechanical Engineering, University of Colorado, Boulder, CO, USA, [11]Department of Physics, University of Toronto, Toronto, ON, Canada, [12]TNO Netherlands Organisation for Applied Scientific Research, The Hague, The Netherlands

Abstract Global trends in tropospheric nitrogen dioxide (NO_2) have changed dramatically in the past decade. Here, we investigate tropospheric NO_2 variabilities over United States, Europe, and E. China in 2005–2018 to explore the mechanisms governing the variation of this critical pollutant. We found large uncertainties in the trends of anthropogenic nitrogen oxides (NO_x) emissions, for example, the reductions of NO_x emissions, derived with different approaches and data sets, are in the range of 35%–50% over the United States and 15%–45% over Europe in 2005–2018. By contrast, the analysis in this work indicates declines of anthropogenic NO_x emissions by about 40% and 25% over the United States and Europe, respectively, in 2005–2018, and about 20% over E. China in 2012–2018. However, the shift of major NO_x sources from power generation to industrial and transportation sectors has led to noticeable diminishing effects in emission controls. Furthermore, satellite measurements exhibit the influence of NO_2 background levels over the United States and Europe, which offset the impacts of anthropogenic emission declines, resulting in flatter trends of tropospheric NO_2 over the United States and Europe. Our analysis further reveals underestimation of background NO_2 by chemical transport models, which can lead to inaccurate interpretations of satellite measurements. We use surface in-situ NO_2 observations to diagnose the satellite-observed NO_2 trends and find top-down NO_x emissions over urban grids represent the changes in anthropogenic NO_x emissions better. This work highlights the importance of comprehensive applications of different analysis approaches to better characterizing atmospheric composition evolution.

Plain Language Summary Nitrogen oxides (NO_x) are one of the important air pollutants and play a key role in the tropospheric environment. Therefore, a correct understanding of the variation of global tropospheric NO_x in recent years seems extremely important. Here, we use different approaches and data sets to obtain the trends of anthropogenic NO_x emissions and explore the mechanisms governing the variation of tropospheric NO_x over the United States, Europe, and E. China during 2005–2018. We found large uncertainties in the trends of anthropogenic NO_x emissions derived with these approaches and data sets, due to the insufficient understanding of real-world reduction efficiencies of emission control technologies and the impacts of non-anthropogenic NO_x changes. After considering these issues, we found significant decreases of anthropogenic NO_x emissions by about 40% and 25% over the United States and Europe in 2005–2018, and about 20% over E. China in 2012–2018. This work highlights the importance of comprehensive applications of different analysis approaches to better characterizing atmospheric composition evolution.

1. Introduction

Fuel consumption associated with industrialization has led to significant variations of pollutant emissions with dramatic changes to atmospheric composition in the past decades (Cooper et al., 2010; Duncan et al., 2016;

Table 1
Reduction Rates and Trends of NO$_2$ Concentrations and NO$_x$ Emissions From Various Data Sets in the United States, Europe and E. China

United states		Reduction rates (2005–2018)	Trends/yr(2005–2010)	Trends/yr(2010–2018)
Bottom-up	EPA NO$_x$	−49.6%	−6.4%	−4.8%
	Fuel-based NO$_x$	−42.4%	−6.4%	−3.3%
Top-down	Continental average	−33.7%	−6.3%	−1.3%
	Urban grids (top 10% OMI NO$_2$)	−41.7%	−7.6%	−2.2%
OMI NO$_2$	Continental average	−36.0%	−7.0%	−1.7%
	Sampled at AQS	−41.0%	−8.9%	−1.9%
Surface NO$_2$	AQS	−42.0%	−6.4%	−3.5%
Europe		**Reduction rates (2005–2018)**	**Trends/yr(2005–2010)**	**Trends/yr(2010–2018)**
Bottom-up	ECLIPSE NO$_x$	−46.1%	−4.7%	−2.9%
	CAO NO$_x$ (temp. adj.)	−28.9% (2005–2015)	−4.1%	−2.3% (2010–2015)
Top-down	Continental average	−15.3%	−3.0%	−0.9%
	Urban grids (top 10% OMI NO$_2$)	−22.4%	−2.9%	−2.3%
OMI NO$_2$	Continental average	−22.8%	−4.2%	−1.2%
	Sampled at Airbase	−31.5%	−4.2%	−2.3%
Surface NO$_2$	Airbase	−27.2%	−2.4%	−2.6%
E.China		**Reduction rates (2012–2018)**	**Trends/yr(2005–2012)**	**Trends/yr(2012–2018)**
Bottom-up	MEIC NO$_x$	−32.8%	5.5%	−5.7%
Top-down	Continental average	−20.2%	3.5%	−3.8%
	Urban grids (top 10% OMI NO$_2$)	−21.7%	2.5%	−4.5%
OMI NO$_2$	Continental average	−31.5%	6.4%	−5.8%
	Sampled at MEE			−3.7% (2014–2018)
Surface NO$_2$	MEE			−1.3% (2014–2018)

Verstraeten et al., 2015; Y. Zhang et al., 2016). As a precursor to ozone (O$_3$) and secondary aerosols, NO$_x$ (= NO + NO$_2$) is one of the most important pollutants and plays a key role in tropospheric chemistry. Sources of tropospheric NO$_x$ include fossil fuel combustion, biomass burning, soil, and lightning emissions. The importance of tropospheric NO$_x$ has made it an essential target of global emission regulations. The successful regulations, employed in the United States and Europe for more than a decade (Crippa et al., 2016; EPA, 2017; EU, 2001; Reis et al., 2012) and China since around 2011 (CSC, 2013; Zheng et al., 2018), have resulted in noticeable decreases of tropospheric NO$_2$ in recent decades in the Northern Hemisphere (Itahashi et al., 2019; Lamsal et al., 2015; Miyazaki et al., 2017; Qu et al., 2020; R. Zhang et al., 2018).

While NO$_x$ emissions are continuously declining in the reported inventories (see Table 1), a recent study (Jiang et al., 2018) reported a marked slowdown in the decrease of tropospheric NO$_2$ over North America since around 2010. The causes for this unexpected change are debated, with differing explanations involving uncertainties in anthropogenic and natural sources, nonlinear response of NO$_2$ columns to emissions, and NO$_x$ lifetime change (Jiang et al., 2018; Laughner & Cohen, 2019; J. Li & Wang, 2019; Qu et al., 2021; Silvern et al., 2019; Song et al., 2021; Wang et al., 2021), illustrating the challenges in understanding tropospheric NO$_2$ variations. This debate points to larger, global-scale questions: are we able to understand the current trends of anthropogenic NO$_x$ emissions, the evolution of tropospheric NO$_2$, and predict their future projections?

As shown in Figure 1, Ozone Monitoring Instrument (OMI) NO$_2$ measurements demonstrate dramatic changes of tropospheric NO$_2$: (a) In 2005–2010, both the United States ($-7.0 \pm 1.0\%$/y) and Europe ($-4.2 \pm 0.7\%$/y) show strong decreases, while E. China shows a strong increase ($5.9 \pm 1.0\%$/y); (b) In 2013–2018, the decreases over the United States ($-2.5 \pm 0.9\%$/y) and Europe ($-1.4 \pm 0.9\%$/y) are much weaker and are contrasted by strong reduction over E. China ($-5.5 \pm 1.2\%$/y). Following Jiang et al. (2018), here we perform a comprehensive analysis
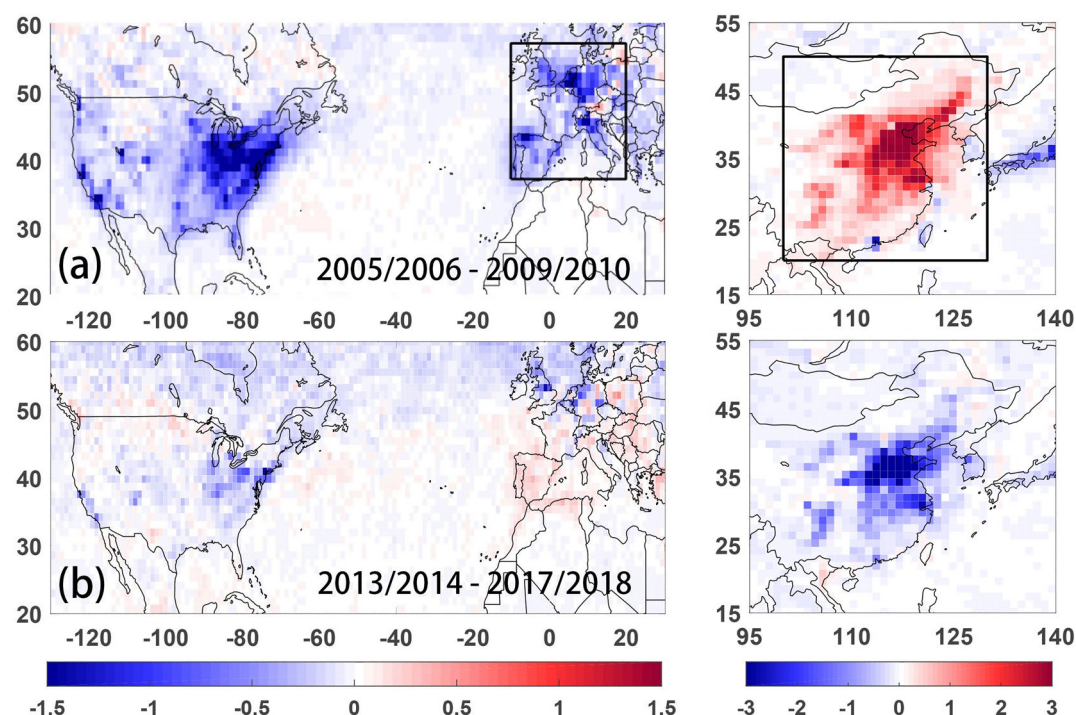
Figure 1. Difference of mean tropospheric OMI NO$_2$ columns from 2005 to 2006 to 2009–2010 (a), and from 2013 to 2014 to 2017–2018 (b). The unit is 10^{15} molec/cm^2. Panel (a) also defines the European and East China domains (land only). The areas outside of China are excluded in the E. China domain.

of tropospheric NO$_2$ variabilities over these three continents in 2005–2018, by combining all available analysis approaches, that is, satellite and surface NO$_2$ measurements, bottom-up and top-down NO$_x$ emission estimates, and chemical transport models to explore the mechanisms governing the variation of this critical pollutant.

2. Data and Methodology

2.1. Bottom-Up NO$_x$ Emission Estimates

2.1.1. EPA NO$_x$ Inventory

The Environmental Protection Agency (EPA) inventory used in this study is from the Air Pollutant Emissions Trends Data. The emissions are updated through the National Emissions Inventory (NEI) 2014v2. The electric generating unit NO$_x$ emissions (2015–2018) were updated to the most recent Clean Air Markets Program Division (CAMD) available data. Mobile emissions in 2018 were calculated using the slope between 2014v2 and the 2017 modeling file.

2.1.2. Fuel-Based NO$_x$ Inventory (United States)

We extend a fuel-based inventory of US NO$_x$ emissions reported in Jiang et al. (2018) through 2018. The effect of the Great Recession is taken into account through drops in on-road diesel activity and on-road gas activity by 3% and 6%, respectively, rather than year-to-year growth. We construct a second emissions case termed the "Fuel-Based NO$_x$ (w/o Dsl Update)." This case is constructed using the fuel-based emissions described in Jiang et al. (2018), except for heavy-duty diesel trucks. Heavy-duty truck emissions are instead substituted using the EPA MOVES2014a model (EPA, 2015). Since 2010, new trucks have been required to install selective catalytic reduction (SCR) systems. Correspondingly, the EPA MOVES model predicts sharp decreases in heavy-duty diesel truck NO$_x$ emissions (2011–2018: approximately 8% y^{-1}). However, recent measurements of in-use vehicles suggest that NO$_x$ emission factors from heavy-duty trucks equipped with SCR systems exceed emission standards by factors of 3–7 (Dixit et al., 2017; Preble et al., 2019; Thiruvengadam et al., 2015). This study relies on in-use

emission factors, which results in heavy-duty diesel NO_x emissions declining twice as slowly (2011–2018: approximately 4% y^{-1}) as in the MOVES model.

2.1.3. ECLIPSE Inventory

The ECLIPSE (Evaluating the Climate and Air Quality Impacts of Short-Lived Pollutants) inventory was developed within the European Union's Seventh Framework Program (Klimont et al., 2017; Stohl et al., 2015). The emission data was created with the GAINS (Greenhouse gas–Air pollution Interactions and Synergies) model (Amann et al., 2011). The historical data for the period 1990–2010 was revised compared to preceding sets using the latest International Energy Agency (IEA), Eurostat and Food and Agriculture Organization (FAO) statistics extending to 2010, as well as country reporting where available. The baseline activity data for the projections originate from the IEA Energy Technology Perspectives study (IEA, 2012) and was extended until 2050 based on current legislation (CLE) scenario (Stohl et al., 2015).

2.1.4. CAO Inventory

The emission estimates used in the Clean Air Outlook (CAO) study (Amann, 2018) were developed with the GAINS model (Amann et al., 2011) and so the overall methodology is comparable to ECLIPSE, that is, a science-based inventory. However, it focuses on the European Union and several updates for European Union countries were made since ECLIPSE: the time series extends to 2015 using latest statistics; revised data on vehicle fleet age and composition were used; information about enforcement of air pollution policies were updated.

2.1.5. MEIC Inventory

The Chinese inventory employed in this study was built under the framework of Multiresolution Emission Inventory for China (MEIC), developed by Tsinghua University (M. Li et al., 2017; Zheng et al., 2018). The MEIC model used the bottom-up approach to estimate anthropogenic emissions from more than 700 source classifications in China, which are aggregated into power, industry, transportation, and residential sectors in the analysis. The activity data are compiled from the provincial energy statistics yearbooks, and the emission factors are dynamically estimated by technology turnover models that track the evolution of manufacturing technologies and pollution control devices over time. For the power sector, the activity data and emission factors are both unit-based parameters, which are used to estimate the emissions from each power plant individually. The NO_x emissions data used in this study are derived from Zheng et al. (2018).

2.2. Top-Down NO_x Emission Estimate

Based on an ensemble Kalman filter technique, Miyazaki et al. (2017) estimated global surface NO_x emissions for the period of 2005–2015 by assimilating multiple satellite data sets. Using the QA4ECV version 1.1 NO_2 products from OMI, SCIAMACHY (SCanning Imaging Absorption spectroMeter for Atmospheric CHartographY) and GOME-2 (Global Ozone Monitoring Experiment 2), updated emission estimates with $1.125° \times 1.125°$ horizontal resolution for 2005–2018 are used in this work, which have been previously used to study processes controlling air quality in East Asia (Miyazaki et al., 2019), and to construct a multi-model, multi-constituent data assimilation analysis (Miyazaki et al., 2020). The combined total (anthropogenic, soil, and lightning) emissions are optimized in data assimilation. This is to avoid the difficulty associated with optimizing the spatiotemporal structure in background errors for each category source separately. In our analysis, individual emission sources were estimated using the emission ratio between different categories in the a priori emission inventories. The forecast model is MIROC-Chem (Watanabe et al., 2011), which considers detailed photochemistry in the troposphere and stratosphere and is coupled to the atmospheric general circulation model MIROC-AGCM version 4. The meteorological fields simulated by MIROC-AGCM were nudged toward the 6-hourly ERA-Interim (Dee et al., 2011).

2.3. Satellite and Surface In-Situ Observations

2.3.1. Tropospheric OMI NO_2 Column Data

The OMI instrument on the Aura satellite has a spatial resolution of 13×24 km (nadir view). OMI provides global coverage with measurements of both direct and atmosphere-backscattered sunlight in the ultraviolet-visible range from 270 to 500 nm; the spectral range 405–465 nm is used to retrieve tropospheric NO_2 columns. The
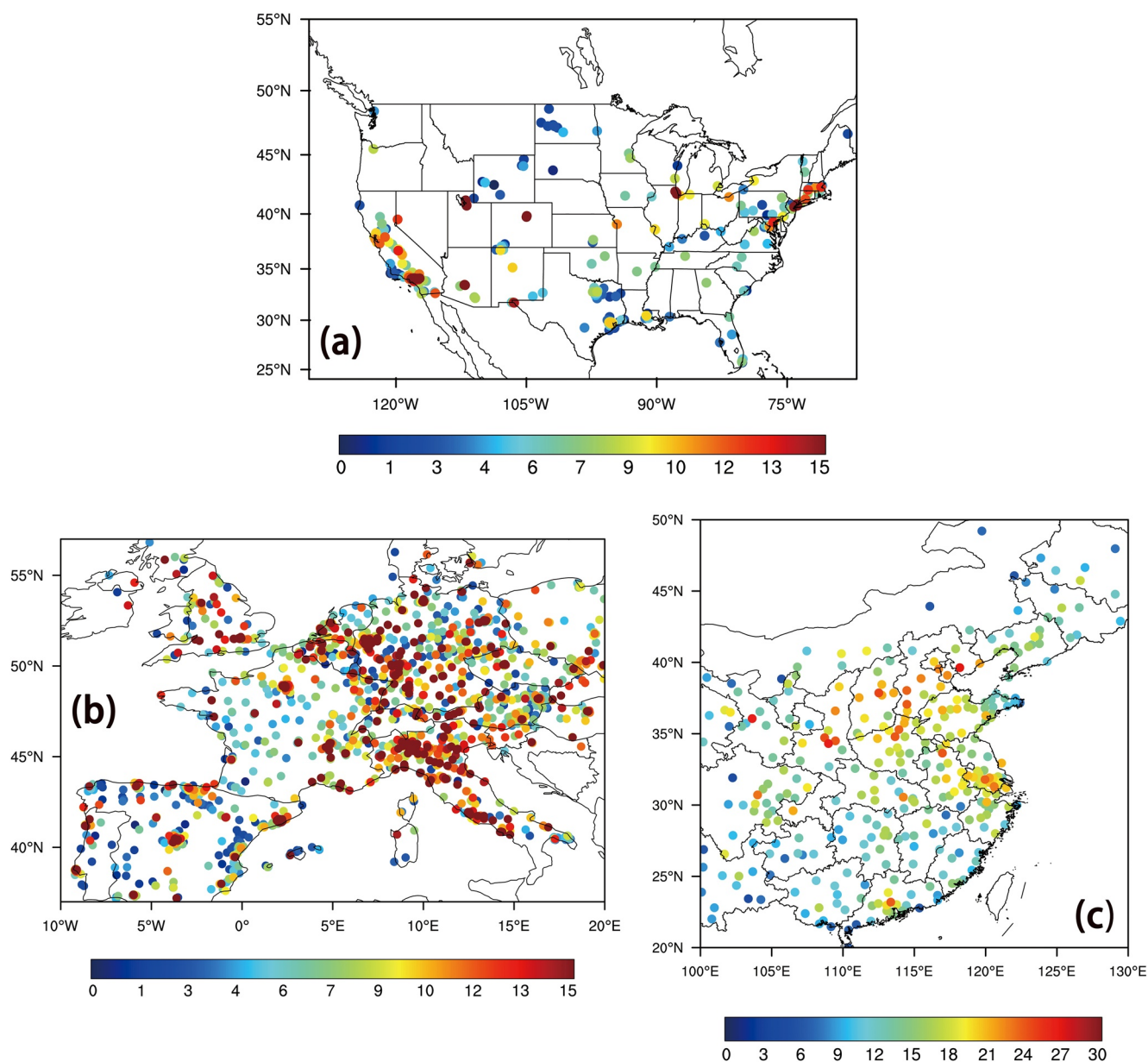
Figure 2. Surface NO$_2$ concentrations (with unit ppb) in 2018 from AQS (a), Airbase (b), and MEE (c) stations used in this work.

OMI retrievals (level 2, QA4ECV (Boersma et al., 2018; Zara et al., 2018)) are used in this work. We refer the reader to Jiang et al. (2018) for the details of OMI NO$_2$ usage.

2.3.2. AQS and AirBase Surface NO$_2$ Measurements

We use in-situ hourly surface NO$_2$ measurements from the US EPA Air Quality System (AQS) network and European Environment Agency (EEA) Airbase networks. The AQS and AirBase networks collect ambient air pollution data from monitoring stations located in urban, suburban, and rural areas. We only considered stations with at least 12-year observation records in 2005–2018. The locations of AQS and AirBase stations used in this work are shown in Figures 2a and 2b. It should be noted that surface NO$_2$ measurements are affected by the interference from other oxidized nitrogen compounds (Lamsal et al., 2015). The interferences in the AQS

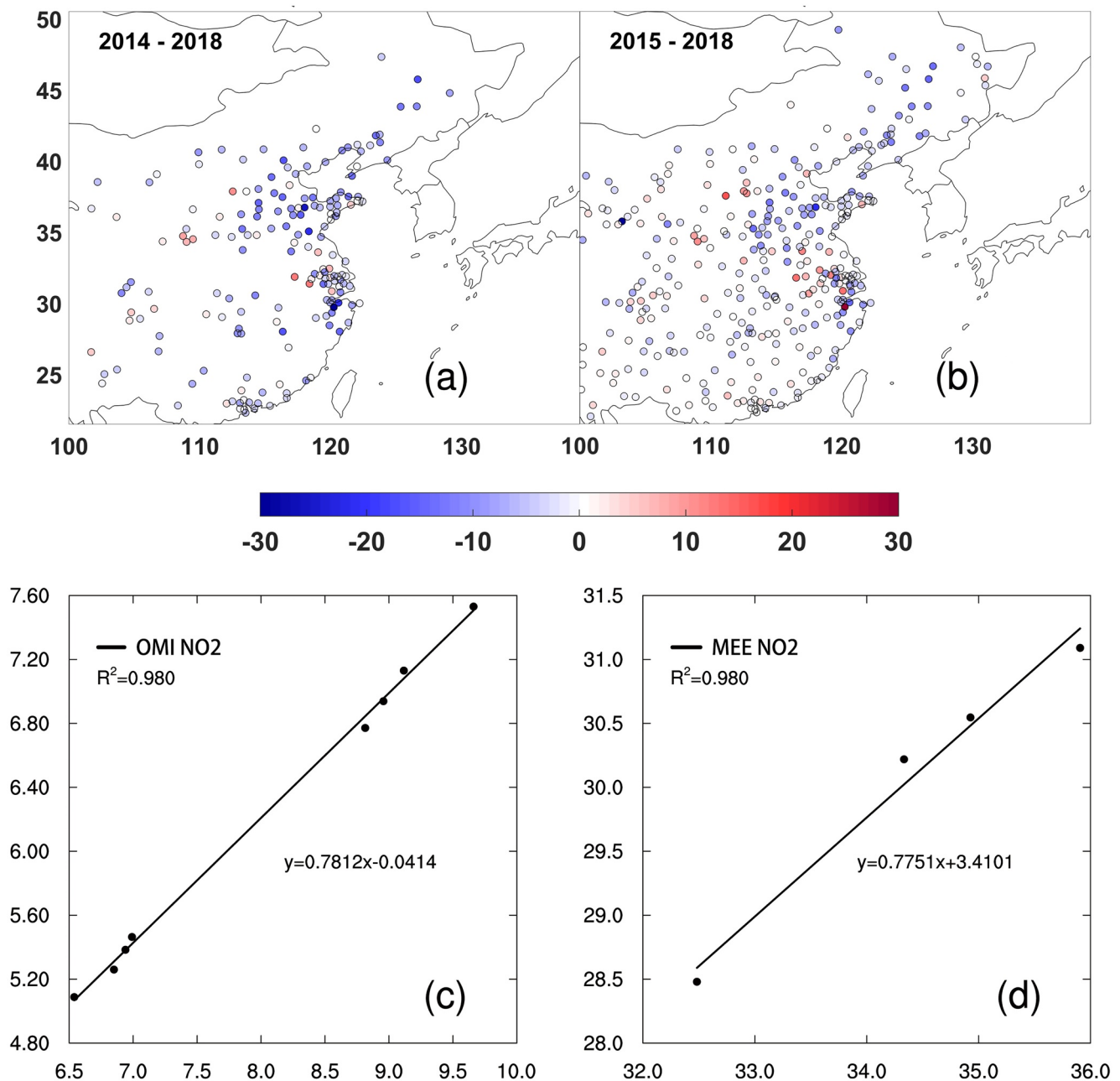**Figure 3.** (a–b) Differences of mean NO$_2$ concentrations of surface in-situ NO$_2$ measurements (MEE) from 2014 to 2018, and from 2015 to 2018. (c) Linear regression relations. *x*-axis: averages of satellite data (2010–2018, excluding 2014) sampled at surface stations in 2014; *y*-axis: averages of satellite data (2015–2018) sampled at surface stations (2015–2018, respectively) and averages of satellite data (2010–2013) sampled at surface stations in 2015 (d) same as panel (c), but for surface NO$_2$ measurements. *x*-axis: averages of surface measurements (2015–2018) of stations collocated with surface stations in 2014; *y*-axis: averages of surface measurements of all available stations in 2015–2018.

and AirBase NO$_2$ observations are not considered in this work, with an assumption of limited influences on the trends.

2.3.3. MEE Surface NO$_2$ Measurements

We collect surface-level NO$_2$ concentration data from the China Ministry of Ecology and Environment (MEE) monitoring network. These real-time monitoring stations can report hourly concentrations of criteria pollutants from over 360 cities in 2018. Figures 3a and 3b show the differences of mean surface NO$_2$ concentrations, as

measured by MEE stations, from 2014 to 2018, and from 2015 to 2018, respectively. While the spatial patterns of the observed difference are consistent, the number of available stations is much smaller in 2014. To remove the effect of representation error due to sparse station distribution in 2014, we adjusted the averages of sampled satellite data in 2014 with the following approach:

1. Sample the satellite data (2010–2018, excluding 2014) at surface stations in 2014, corresponding to variable "x" in Figure 3c
2. Sample the satellite data (2015–2018) at surface stations (2015–2018, respectively); Sample the satellite data (2010–2013) at surface stations in 2015; corresponding to variable "y" in Figure 3c
3. Get the linear regression relation: $y = ax + b$
4. Get the adjusted value for the 2014 data: $C_{2014\_adjusted} = aC_{2014} + b$

As shown in Figure 3c, the scarcity of surface stations in 2014 resulted in (biased) high NO_2 concentrations, because most stations in 2014 are located in highly polluted urban areas. Besides satellite data, the average of surface in-situ NO_2 measurements in 2014 is adjusted with a similar approach, as described in Figure 3d. Similar to AQS and AirBase NO_2 observations, the interference from other oxidized nitrogen on MEE NO_2 observations (Liu et al., 2018) are not considered in this work.

2.4. GEOS-Chem Model Simulations

The GEOS-Chem chemical transport model (http://www.geos-chem.org, version 12-8-1) is driven by assimilated meteorological data of MERRA-2 with nested $0.5° \times 0.625°$ horizontal resolution. The GEOS-Chem model includes fully coupled O_3-NO_x-VOC-halogen-aerosol chemistry. The chemical boundary conditions are updated every 3 h from a global simulation with $4° \times 5°$ resolution. Emissions in GEOS-Chem are computed by the Harvard-NASA Emission Component (HEMCO). We refer the reader to X. Chen et al. (2021) for the details of model configurations.

3. Results and Discussions

3.1. Trends of US NO_x Emissions

Figure 4a provides an extended analysis for U.S. anthropogenic NO_x emissions based on Jiang et al. (2018). Tropospheric OMI NO_2 columns are assimilated with the same ensemble Kalman filter approach in Jiang et al. (2018) to produce an updated estimate of top-down NO_x emissions. Figure 4a shows the trends of US EPA's NO_x emission inventory (black line) (EPA, 2019), revised bottom-up NO_x emissions with a fuel-based approach to estimate mobile/stationary/area sources (green lines), and top-down anthropogenic NO_x emissions (magenta line). The red line shows U.S. AQS surface NO_2 measurements, and the blue line shows OMI NO_2 measurements. The difference between EPA's inventory (black line) and revised fuel-based inventory (green solid line) can be explained by updating heavy-duty diesel truck emission factors based on real-world measurements (i.e., the difference between green solid and dashed lines), raising questions about the anticipated effectiveness of selective catalytic reduction (SCR) systems (Y. Chen et al., 2020; Dixit et al., 2017; Preble et al., 2019; Thiruvengadam et al., 2015).

3.2. Trends of European NO_x Emissions

Figure 4b (black line) shows the trend of European anthropogenic NO_x emissions (ECLIPSE inventory). The total reductions of TNO-MACC (Netherlands Organisation for Applied Scientific Research—Monitoring Atmospheric Composition and Climate), EEA, Hoesly et al. (2018), and United Nations Economic Commission for Europe (UNECE) inventories are broadly consistent with ECLIPSE (Figure S1 in Supporting Information S1). Similar to the United States, the inventories representing official estimates show systematically a more optimistic picture than the science-based inventories (ECLIPSE, TNO-MACC; Hoesly et al. (2018), see Supporting Information S1) since 2010. A more in-depth analysis shows that officially reported data assumes much smaller impacts of "dieselgate": in the EEA and UNECE data, emissions from diesel cars and light-duty vehicles decrease by about 20% between 2005 and 2010 and continue to decline slightly thereafter, whereas
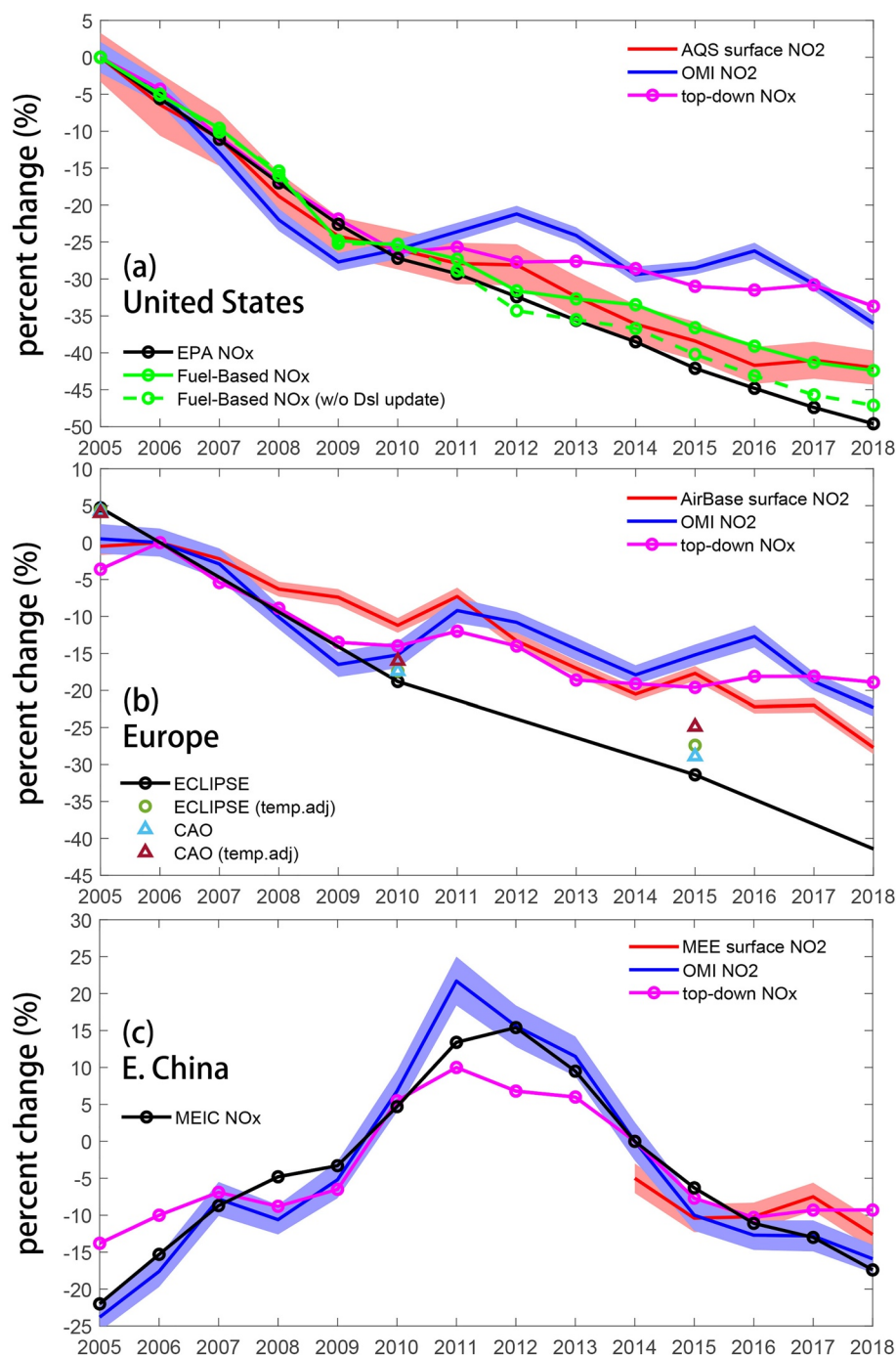
Figure 4. (a) Percent changes (normalized at 2005) of AQS surface NO_2 measurements, tropospheric OMI NO_2 columns, and U.S. anthropogenic NO_x emissions including: top-down, bottom-up (EPA); revised bottom-up with a fuel-based approach, revised bottom-up without diesel NO_x update. (b) Percent changes (normalized at 2006) of AirBase surface NO_2 measurements, OMI NO_2, and European anthropogenic NO_x emissions, including: top-down, ECLIPSE, adjusted ECLIPSE by considering the effect of temperature; CAO and adjusted CAO. The ECLIPSE and CAO data are available every 5 years. (c) Percent changes (normalized at 2014) of MEE surface NO_2 measurements, OMI NO_2, and E. China anthropogenic NO_x emissions including: top-down, MEIC. The shaded areas represent 1-sigma uncertainties for random and sampling errors, calculated with the bootstrapping method (Jiang et al., 2018).
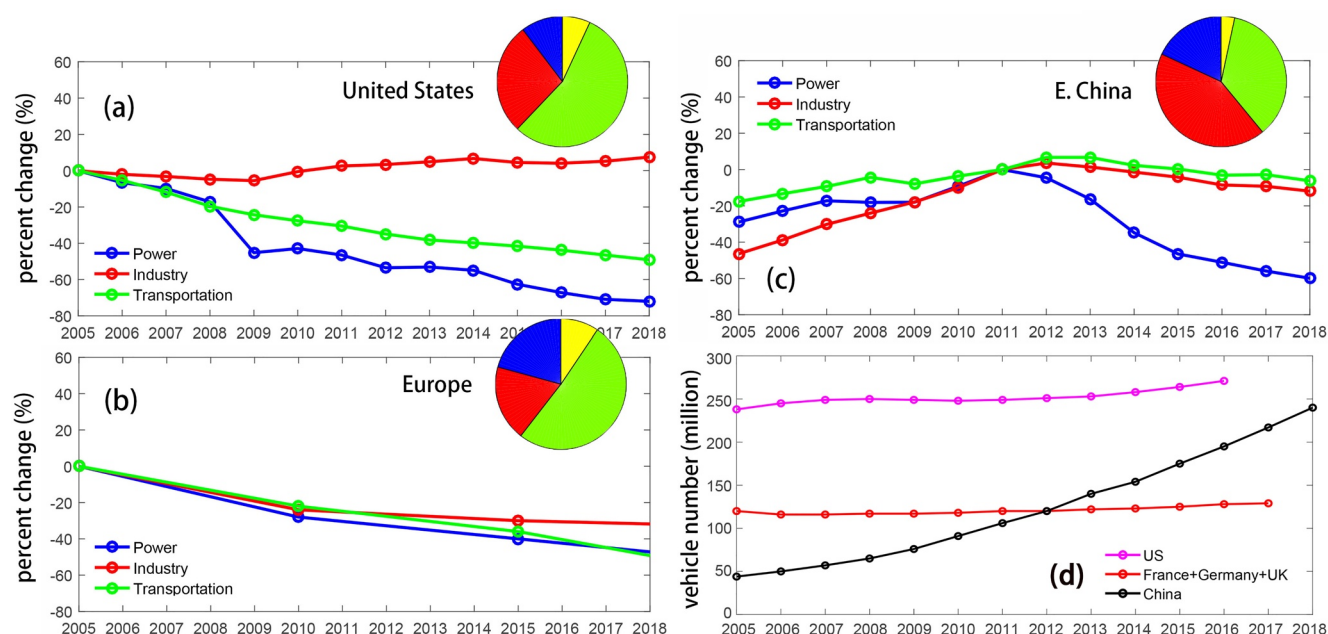
Figure 5. (a–b) Percent changes (normalized at 2005) of anthropogenic NO_x emissions from power generation, industrial and transportation sectors for the United States (revised bottom-up) and Europe (ECLIPSE). The pie charts show the fractions of each sector in 2018: power (blue), industry (red), transportation (green), and others (yellow). (c) Same as panels (a–b), but for E. China (MEIC) normalized at 2011. (d) Changes of total vehicle number from 2005 to 2018 for the United States, France + Germany + United Kingdom, and China.

they remain constant or even increase in the ECLIPSE to account for defeat devices employed under real-world driving.

A more recent study (clean air outlook—CAO) where the same model was used as for ECLIPSE, but statistics and policies were updated, shows a slightly lower reduction in NO_x by 2015, that is, about 28% compared to about 31% in the ECLIPSE. Similar to questions about the effectiveness of SCR systems on heavy-duty trucks in the United States under lower engine temperatures, recent research has shown that light-duty diesel vehicle NO_x emission factors are higher under colder ambient temperatures (Sjodin, 2018). Considering the reanalyzed effect of temperature on diesel vehicles could result in a further decline in the reduction rate (estimated in CAO) to about 24%. Unlike the U.S. passenger vehicles which are almost entirely powered by gasoline, a higher fraction of light-duty vehicles in Europe are powered by diesel in addition to heavy-duty trucks. Therefore, it is expected that elevated NO_x emissions associated with diesel vehicles will be more pronounced in Europe than in the United States, resulting in slower decreases in NO_x emissions.

3.3. Trends of Chinese NO_x Emissions

Figure 4c shows the trends of MEIC (black line), top-down (magenta line) Chinese anthropogenic NO_x emissions, and MEE network surface NO_2 measurements (red line). The increasing trend of Chinese NO_x emissions has been reversed since around 2011 due to the successful emission regulations. Figure 5c shows the trends of anthropogenic NO_x emissions in China from power generation, industrial, and transportation sectors in the MEIC inventory. To meet the "ultralow" emission standard for power plants, SCR systems have been increasingly installed in utilities for coal-fired power plants with a penetration rate of >95% by 2017 (Zheng et al., 2018). The installation of new clean devices resulted in a dramatic decrease of NO_x emissions from power plants by 16%/y in 2011–2015, with diminishing effects afterward, that is, the reduction rate is 5%/y in 2015–2018 (Figure 5c). The total reduction rates of NO_x emissions from the power sector are comparable between the United State (72%, 2005–2018) and China (60%, 2011–2018).

Within the same period (2011-2018), the reduction rates for industry and transportation sectors are as low as 2%/y and 1%/y (Figure 5c), respectively. Industry emission standards have been strengthened since 2013, but it seems they have had limited influences on the total emissions since only the cement industry widely applied NO_x

control technologies. For the transportation sector, a series of measures such as strengthening vehicle emissions standards, retiring old vehicles, and improving fuel quality were adopted. However, the efforts to control vehicle emissions are offset by the rising vehicle number and the weaker emission limits on the off-road diesel engines (Zheng et al., 2018). As shown in Figure 5d, the number of vehicles in China increased from 44 million to 240 million in 2005–2018 (MPSC, 2018). On the contrary, the small changes in vehicle numbers (Figures 5a and 5b) lead to much stronger declines in vehicle emissions from the United States and Europe (TEDB, 2021).

The above analyses indicate that the major driver of NO_x emission reductions has shifted from power generation to industrial and transportation sources over North America, Europe, and East Asia. The transportation and industrial sectors together contribute about 83%, 70%, and 79% of anthropogenic NO_x emissions in the United States, Europe, and China in 2018 (Figure 5), respectively. Continuous steep reductions are not expected because large sources (power sector) have been well controlled, and a large number of smaller combustion sources (industry and transport sectors) are more challenging to control. In addition, an important theme is the importance of the transportation sector on anthropogenic emission trends, which now comprise 36%–55% of the anthropogenic NO_x emissions across the three continents (Figures 5a–5c). As discussed, the transportation emission trends are most affected by: (a) heavy-duty diesel trucks in the United States; (b) light-duty diesel vehicles in Europe; (c) rapid growth in passenger vehicles in China. In particular, the situation could be dire for air quality in China: according to China's National Information Center, China's vehicle number is expected to reach 280 million by 2020, 360 million by 2025, and the peak of car ownership will be 600 million. The growing importance of transportation in China poses a significant barrier to reducing anthropogenic NO_x in the near future. To put this in perspective, the current number of vehicles in the United States, United Kingdom, Germany, and France combined is about 400 million (Figure 5d).

3.4. Changes in the NO_2 Background

The consistency between updated anthropogenic NO_x emissions and surface NO_2 measurements (Figures 4a and 4b and Table 1), that is, $-3.3 \pm 0.2\%$/y (fuel-based inventory) and $-3.5 \pm 0.3\%$/y (AQS NO_2) over the United States in 2010–2018; -2.3%/y (adjusted CAO in 2010–2015) and $-2.6 \pm 0.8\%$/y (Airbase NO_2) over Europe in 2010–2018, indicates the feasibility of evaluating NO_x emission trends with surface NO_2 measurements. However, they are not sufficient to explain the observed flatter trends of tropospheric NO_2 columns, as well as top-down NO_x based on satellite measurements (Figures 4a and 4b and Table 1), that is, $-1.7 \pm 0.5\%$/y (OMI NO_2) and $-1.3 \pm 0.2\%$/y (top-down NO_x) over the United States; $-1.2 \pm 0.5\%$/y (OMI NO_2) and $-0.9 \pm 0.3\%$/y (top-down NO_x) over Europe in 2010–2018.

Figure 6 (blue dashed lines) shows OMI tropospheric NO_2 columns, sampled at locations and times of surface measurements. In contrast to the continental averages (blue solid lines), the sampled satellite measurements match better with surface observations, confirming the reliability of NO_2 observation records provided by OMI, as well as the small influence from other oxidized nitrogen compounds (Lamsal et al., 2015; Liu et al., 2018) on the derived NO_2 trends. Because the density of surface stations (and sampled OMI measurements) is higher over polluted areas, the sampled OMI NO_2 are more strongly affected by local anthropogenic emissions; in contrast, the continental averaged OMI NO_2 are less affected by local anthropogenic emissions (Qu et al., 2021; Silvern et al., 2019; Song et al., 2021; Wang et al., 2021). The discrepancies between continental averaged and sampled OMI NO_2 thus, represent changes of NO_2 background from nonlocal sources, such as natural sources and possible intercontinental pollution transport (Qu et al., 2021; Silvern et al., 2019). We didn't find a noticeable change in NO_2 background over E. China (Figure 6c). It is possible that future NO_2 background change in China could become observable when longer surface observation records become available.

3.5. Impacts on Derived Anthropogenic NO_x Emissions

Figure 7 (magenta dashed lines) shows surface NO_2 concentrations from GEOS-Chem model, sampled at locations and times of surface measurements. The total anthropogenic NO_x and VOCs emissions in the GEOS-Chem model are scaled with the corresponding bottom-up inventories (EPA, ECLIPSE, and MEIC). The consistency between modeled surface NO_2 and bottom-up inventories indicates that surface NO_2 observations can represent the trends of anthropogenic NO_x emissions, which reaffirms the feasibility of evaluating NO_x emission trends with surface NO_2 measurements. The good agreements among updated anthropogenic emissions, surface and
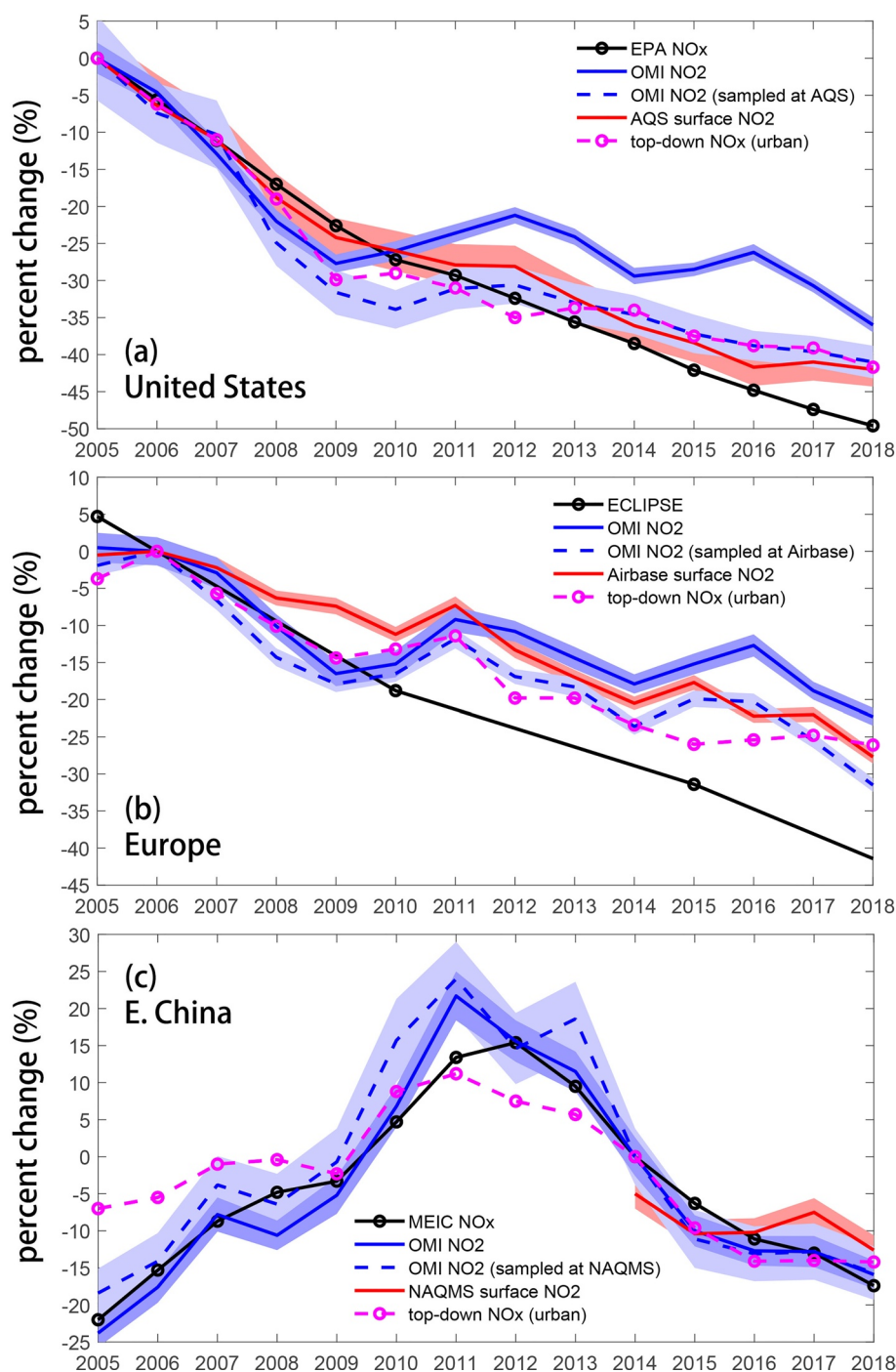
Figure 6. Percent changes of bottom-up inventories (EPA, ECLIPSE, and MEIC), top-down NO_x (urban grids), surface NO_2 measurements (AQS, AirBase, and MEE), tropospheric OMI NO_2 columns, and OMI NO_2 sampled at locations and times of surface measurements for U.S. (a), Europe (b) and E. China (c), respectively. For E. China, the satellite data (2005–2013) is sampled at surface stations in 2015.

sampled satellite measurements (Figures 4a and 4b; Figures 6a and 6b) further suggest that the reductions of tropospheric NO_2 over polluted areas are dominated by anthropogenic emission changes. For example, declines over the United States in 2005–2018 are about 41%–42% (Table 1) in updated anthropogenic NO_x emissions (green solid line in Figure 4a), AQS surface NO_2 measurements (red line in Figure 4a) and OMI NO_2 sampled at AQS
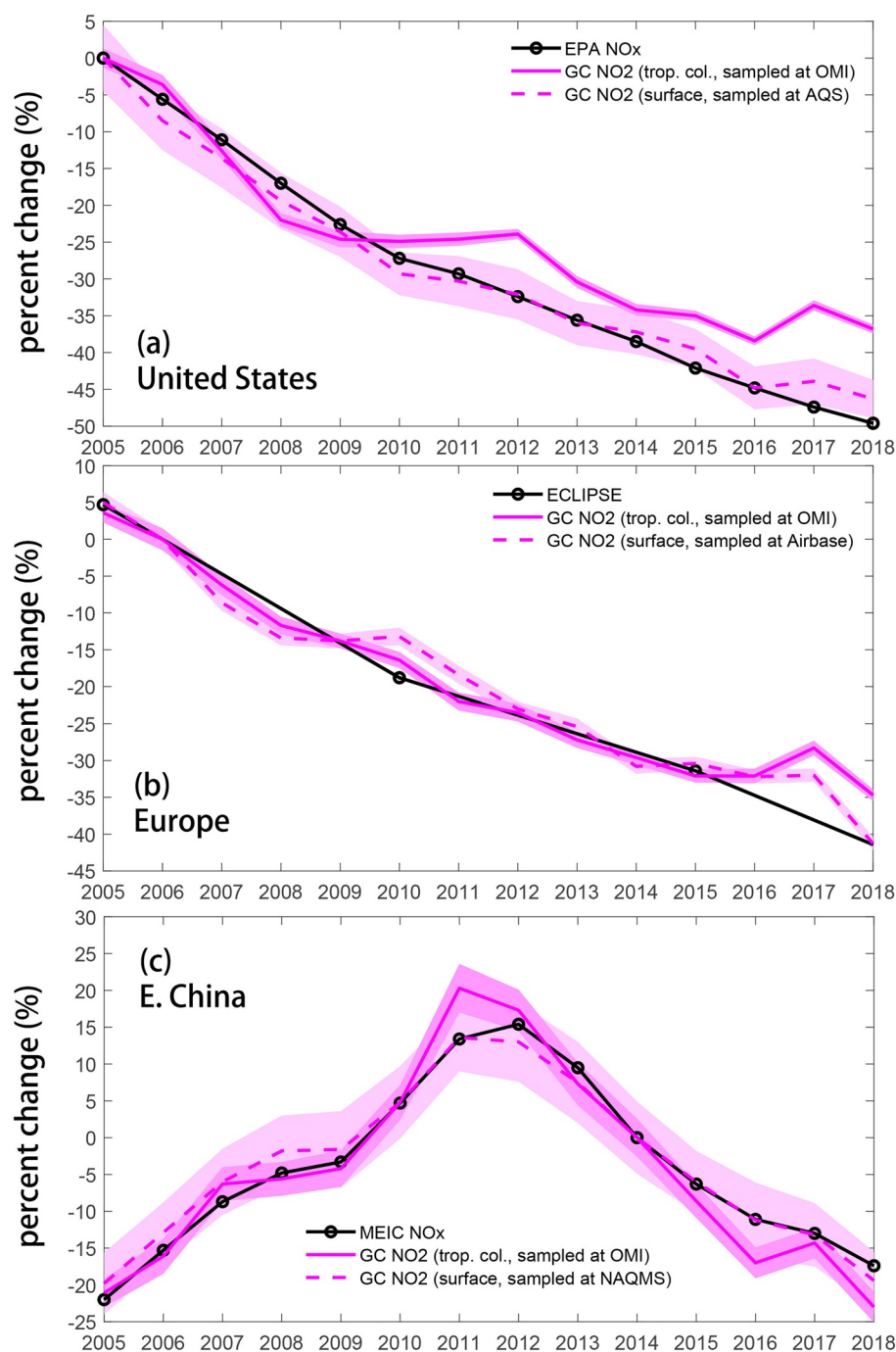
Figure 7. Percent changes of bottom-up inventories (EPA, ECLIPSE, and MEIC), modeled surface NO_2 sampled at locations and times of surface measurements and modeled tropospheric NO_2 columns sampled at locations and times of OMI NO_2 measurements for U.S. (a), Europe (b) and E. China (c), respectively. The total anthropogenic NO_x and VOCs emissions in the GEOS-Chem model ($0.5° \times 0.625°$ horizontal resolution) are scaled with the corresponding bottom-up inventories (EPA, ECLIPSE, and MEIC). For E. China, the modeled surface NO_2 (2005–2013) is sampled at surface stations in 2015.

measurements (blue dashed line in Figure 6a). The consistent changes between tropospheric NO_2 and anthropogenic NO_x emissions imply limited variability of tropospheric NO_2 lifetimes in 2005–2018.

Furthermore, Figure 7 (magenta solid lines) shows modeled tropospheric NO_2 columns, sampled at locations and times of OMI NO_2 measurements (continental averages). The difference between solid and dashed magenta lines

in Figure 7a demonstrates the significant contributions from background NO_2 over the United States in the period of 2009–2018, although the magnitude is smaller than observations (Figure 6a). In addition, the GEOS-Chem model suggests consistent trends between tropospheric NO_2 columns and surface NO_2 concentrations over Europe and E. China (Figures 7b and 7c), despite the contributions from background NO_2 over Europe shown by Figure 6b. The underestimation of NO_2 background changes over the United States and Europe were projected into the derived continental averaged anthropogenic emissions (Figures 4a and 4b): the top-down NO_x (magenta lines) follow continental averages of satellite measurements (blue lines) instead of surface NO_2 measurements (red lines). However, as shown in Figure 6, the top-down NO_x over urban grids (i.e., grids with top 10% of mean tropospheric OMI NO_2 columns in 2005–2018, magenta dashed lines in Figure 6) show better agreements with sampled satellite measurements (blue dashed lines) and surface observations (red lines) in the United States and Europe. Consequently, satellite-based top-down NO_x emissions over urban grids can provide better representation for the changes in anthropogenic NO_x emissions, while the trends in the continental averaged anthropogenic NO_x emissions may be biased due to the impacts from NO_2 backgrounds.

4. Conclusions

There are large uncertainties in the derived trends of anthropogenic NO_x emissions. For example, Figure 4 shows that the reductions of NO_x emissions, derived with different approaches and data sets, are in the range of 35%–50% over the United States and 15%–45% over Europe in 2005–2018 (Table 1). The uncertainties, as shown in this work, are caused by insufficient understanding of real-world reduction efficiencies of emission control technologies, as well as the impacts of NO_2 background changes, which pose a significant barrier to characterizing present and future atmospheric chemical composition. The comprehensive analysis in this work indicates significant declines of anthropogenic NO_x emissions by about 40% and 25% over the United States and Europe in 2005–2018, and about 20% over E. China in 2012–2018, approximately (based on top-down NO_x emissions over urban grids). However, the shift of major NO_x sources from power generation to industrial and transportation sectors has coincided with noticeable diminishing effects in emission controls. For example, the trends of anthropogenic NO_x emissions are $-6.4 \pm 0.5\%$/y and $-3.3 \pm 0.2\%$/y (fuel-based inventory) over the United States and -4.1%/y and -2.3%/y (CAO temp. adj.) over Europe before and after 2010 (Table 1). Past trends are unlikely to be predictive of future projections of global NO_x emissions, which will affect trends in surface air quality as well as future scenarios with ambitious mitigation goals that are used in modeling and decision making.

Furthermore, satellite measurements exhibit significant NO_2 background levels over the United States and Europe, which offset the impacts of anthropogenic emission declines, and resulted in flatter trends of tropospheric NO_2 over the United States and Europe in 2010–2018. The good agreements among updated anthropogenic emissions, surface and sampled satellite measurements further suggest small influence from other oxidized nitrogen compounds (Lamsal et al., 2015; Liu et al., 2018) on the derived NO_2 trends, as well as limited variability of tropospheric NO_2 lifetimes over polluted areas in 2005–2018, despite more investigation is needed according to recent analyses (Shah et al., 2020; Zara et al., 2021). While the chemical transport model reproduced higher background NO_2 levels over the United States, the modeled magnitudes of NO_2 background changes are underestimated, which resulted in the inaccurate interpretation of satellite measurements, that is, stagnant NO_x emission reductions instead of continuous declines. By contrast, top-down anthropogenic NO_x emissions over urban grids can provide better representation for the changes in anthropogenic NO_x emissions. Comprehensive applications of satellite and surface NO_2 observations, to constrain emissions in polluted and background areas respectively, are expected to provide more accurate estimations for NO_x emission changes.

Data Availability Statement

The AQS and AirBase surface NO_2 data can be downloaded from: https://www.eea.europa.eu/data-and-maps/data/aqereporting-8 and https://aqs.epa.gov/aqsweb/airdata/download_files.html#Row. The OMI tropospheric NO_2 column data can be downloaded from https://www.temis.nl/airpollution/no2.php. The EPA NO_x inventory can be downloaded at https://www.epa.gov/air-emissions-inventories/air-pollutant-emissions-trends-data. The ECLIPSE inventory can be downloaded at http://www.iiasa.ac.at/web/home/research/researchPrograms/air/ECLIPSEv5a.html. The source code and run directories for model simulations, top-down NO_x, summary of European inventory data and MEE surface NO_2 data can be downloaded from http://doi.org/10.5281/zenodo.5031338.

References

Amann, M. (2018). *Progress towards the achievement of the EU's air quality and emissions objectives*. IIASA.

Amann, M., Bertok, I., Borken-Kleefeld, J., Cofala, J., Heyes, C., Höglund-Isaksson, L., et al. (2011). Cost-effective control of air quality and greenhouse gases in Europe: Modeling and policy applications. *Environmental Modelling & Software*, *26*(12), 1489–1501. https://doi.org/10.1016/j.envsoft.2011.07.012

Boersma, K. F., Eskes, H. J., Richter, A., De Smedt, I., Lorente, A., Beirle, S., et al. (2018). Improving algorithms and uncertainty estimates for satellite NO_2 retrievals: Results from the quality assurance for the essential climate variables (QA4ECV) project. *Atmospheric Measurement Techniques*, *11*(12), 6651–6678. https://doi.org/10.5194/amt-11-6651-2018

Chen, X., Jiang, Z., Shen, Y., Li, R., Fu, Y., Liu, J., et al. (2021). Chinese regulations are working - why is surface ozone over industrialized areas still high? Applying lessons from Northeast US air quality evolution. *Geophysical Research Letters*, *48*, e2021GL092816.

Chen, Y., Sun, R., & Borken-Kleefeld, J. (2020). On-road NO_x and smoke emissions of diesel light commercial vehicles-combining remote sensing measurements from across Europe. *Environmental Science & Technology*, *54*(19), 11744–11752. https://doi.org/10.1021/acs.est.9b07856

Cooper, O. R., Parrish, D. D., Stohl, A., Trainer, M., Nédélec, P., Thouret, V., et al. (2010). Increasing springtime ozone mixing ratios in the free troposphere over western North America. *Nature*, *463*(7279), 344–348. https://doi.org/10.1038/nature08708

Crippa, M., Janssens-Maenhout, G., Dentener, F., Guizzardi, D., Sindelarova, K., Muntean, M., et al. (2016). Forty years of improvements in European air quality: Regional policy-industry interactions with global impacts. *Atmospheric Chemistry and Physics*, *16*(6), 3825–3841. https://doi.org/10.5194/acp-16-3825-2016

CSC. (2013). *China state council: Action plan on prevention and control of air pollution*.

Dee, D. P., Uppala, S. M., Simmons, A. J., Berrisford, P., Poli, P., Kobayashi, S., et al. (2011). The ERA-interim reanalysis: Configuration and performance of the data assimilation system. *Quarterly Journal of the Royal Meteorological Society*, *137*(656), 553–597.

Dixit, P., Miller, J. W., Cocker, D. R., Oshinuga, A., Jiang, Y., Durbin, T. D., & Johnson, K. C. (2017). Differences between emissions measured in urban driving and certification testing of heavy-duty diesel engines. *Atmospheric Environment*, *166*, 276–285. https://doi.org/10.1016/j.atmosenv.2017.06.037

Duncan, B. N., Lamsal, L. N., Thompson, A. M., Yoshida, Y., Lu, Z., Streets, D. G., et al. (2016). A space-based, high-resolution view of notable changes in urban NO_x pollution around the world (2005-2014). *Journal of Geophysical Research: Atmospheres*, *121*(2), 976–996. https://doi.org/10.1002/2015jd024121

EPA. (2015). *MOVES2014a (Motor vehicle emission simulator), office of transportation and air quality*. U.S. Environmental Protection Agency.

EPA. (2017). *United States environmental protection agency: Overview of the clean air Act and air pollution*.

EPA. (2019). *United States environmental protection agency: NEI 2014, air pollutant emissions trends data*.

EU. (2001). *Proposal for a directive of the European Parliament and of the council on the reduction of national emissions of certain atmospheric pollutants and amending Directive 2003/35/EC*.

Hoesly, R. M., Smith, S. J., Feng, L., Klimont, Z., Janssens-Maenhout, G., Pitkanen, T., et al. (2018). Historical (1750–2014) anthropogenic emissions of reactive gases and aerosols from the Community Emissions Data System (CEDS). *Geoscientific Model Development*, *11*(1), 369–408. https://doi.org/10.5194/gmd-11-369-2018

IEA. (2012). *Energy technology perspectives 2012: Pathways to a clean energy system*.

Itahashi, S., Yumimoto, K., Kurokawa, J.-i., Morino, Y., Nagashima, T., Miyazaki, K., et al. (2019). Inverse estimation of NO_x emissions over China and India 2005–2016: Contrasting recent trends and future perspectives. *Environmental Research Letters*, *14*(12), 124020 https://doi.org/10.1088/1748-9326/ab4d7f

Jiang, Z., McDonald, B. C., Worden, H., Worden, J. R., Miyazaki, K., Qu, Z., et al. (2018). Unexpected slowdown of US pollutant emission reduction in the past decade. *Proceedings of the National Academy of Sciences of the United States of America*, *115*(20), 5099–5104. https://doi.org/10.1073/pnas.1801191115

Klimont, Z., Kupiainen, K., Heyes, C., Purohit, P., Cofala, J., Rafaj, P., et al. (2017). Global anthropogenic emissions of particulate matter including black carbon. *Atmospheric Chemistry and Physics*, *17*(14), 8681–8723. https://doi.org/10.5194/acp-17-8681-2017

Lamsal, L. N., Duncan, B. N., Yoshida, Y., Krotkov, N. A., Pickering, K. E., Streets, D. G., & Lu, Z. (2015). U.S. NO_2 trends (2005–2013): EPA air quality system (AQS) data versus improved observations from the ozone monitoring instrument (OMI). *Atmospheric Environment*, *110*, 130–143. https://doi.org/10.1016/j.atmosenv.2015.03.055

Laughner, J. L., & Cohen, R. C. (2019). Direct observation of changing NO_x lifetime in North American cities. *Science*, *366*(6466), 723–727. https://doi.org/10.1126/science.aax6832

Li, J., & Wang, Y. (2019). Inferring the anthropogenic NO_x emission trend over the United States during 2003–2017 from satellite observations: Was there a flattening of the emission trend after the Great Recession? *Atmospheric Chemistry and Physics*, *19*(24), 15339–15352. https://doi.org/10.5194/acp-19-15339-2019

Li, M., Zhang, Q., Kurokawa, J.-i., Woo, J.-H., He, K., Lu, Z., et al. (2017). Mix: A mosaic Asian anthropogenic emission inventory under the international collaboration framework of the MICS-Asia and HTAP. *Atmospheric Chemistry and Physics*, *17*(2), 935–963. https://doi.org/10.5194/acp-17-935-2017

Liu, F., Ronald, J. V., Eskes, H., Ding, J. Y., & Mijling, B. (2018). Evaluation of modeling NO_2 concentrations driven by satellite-derived and bottom-up emission inventories using in situ measurements over China. *Atmospheric Chemistry and Physics*, *18*(6), 4171–4186. https://doi.org/10.5194/acp-18-4171-2018

Miyazaki, K., Bowman, K. W., Yumimoto, K., Walker, T., & Sudo, K. (2020). Evaluation of a multi-model, multi-constituent assimilation framework for tropospheric chemical reanalysis. *Atmospheric Chemistry and Physics*, *20*(2), 931–967. https://doi.org/10.5194/acp-20-931-2020

Miyazaki, K., Eskes, H., Sudo, K., Boersma, K. F., Bowman, K., & Kanaya, Y. (2017). Decadal changes in global surface NO_x emissions from multi-constituent satellite data assimilation. *Atmospheric Chemistry and Physics*, *17*(2), 807–837. https://doi.org/10.5194/acp-17-807-2017

Miyazaki, K., Sekiya, T., Fu, D., Bowman, K. W., Kulawik, S. S., Sudo, K., et al. (2019). Balance of emission and dynamical controls on ozone during the Korea-United States air quality Campaign from Multiconstituent satellite data assimilation. *Journal of Geophysical Research: Atmospheres*, *124*(1), 387–413. https://doi.org/10.1029/2018jd028912

MPSC. (2018). *The Ministry of Public Security of China: National Motor vehicles and drivers Maintain high growth in 2017*.

Preble, C. V., Harley, R. A., & Kirchstetter, T. W. (2019). Control technology-driven changes to in-use heavy-duty diesel truck emissions of nitrogenous Species and related environmental impacts. *Environmental Science & Technology*, *53*(24), 14568–14576. https://doi.org/10.1021/acs.est.9b04763

Qu, Z., Henze, D. K., Cooper, O. R., & Neu, J. L. (2020). Impacts of global NO_x inversions on NO_2 and ozone simulations. *Atmospheric Chemistry and Physics*, *20*(21), 13109–13130. https://doi.org/10.5194/acp-20-13109-2020

Qu, Z., Jacob, D. J., Silvern, R. F., Shah, V., Campbell, P. C., Valin, L. C., & Murray, L. T. (2021). US COVID-19 shutdown demonstrates importance of background NO_2 in inferring NO_x emissions from satellite NO_2 observations. *Geophysical Research Letters*, *48*(10). e2021GL092783 https://doi.org/10.1029/2021gl092783

Reis, S., Grennfelt, P., Klimont, Z., Amann, M., ApSimon, H., Hettelingh, J.-P., et al. (2012). Atmospheric science. From acid rain to climate change. *Science*, *338*(6111), 1153–1154. https://doi.org/10.1126/science.1226514

Shah, V., Jacob, D. J., Li, K., Silvern, R. F., Zhai, S., Liu, M., et al. (2020). Effect of changing NO_x lifetime on the seasonality and long-term trends of satellite-observed tropospheric NO_2 columns over China. *Atmospheric Chemistry and Physics*, *20*(3), 1483–1495. https://doi.org/10.5194/acp-20-1483-2020

Silvern, R. F., Jacob, D. J., Mickley, L. J., Sulprizio, M. P., Travis, K. R., Marais, E. A., et al. (2019). Using satellite observations of tropospheric NO_2 columns to infer long-term trends in US NO_x emissions: The importance of accounting for the free tropospheric NO_2 background. *Atmospheric Chemistry and Physics*, *19*(13), 8863–8878. https://doi.org/10.5194/acp-19-8863-2019

Sjodin, A. e. a. (2018), Real-driving emissions from diesel passenger cars measured by remote sensing and as compared with PEMS and chassis dynamometer measurements - $CONO_x$ Task 2 report.

Song, W., Liu, X.-Y., Hu, C.-C., Chen, G.-Y., Liu, X.-J., Walters, W. W., et al. (2021). Important contributions of non-fossil fuel nitrogen oxides emissions. *Nature Communications*, *12*(1). 1-7. https://doi.org/10.1038/s41467-020-20356-0

Stohl, A., Aamaas, B., Amann, M., Baker, L. H., Bellouin, N., Berntsen, T. K., et al. (2015). Evaluating the climate and air quality impacts of short-lived pollutants. *Atmospheric Chemistry and Physics*, *15*(18), 10529–10566. https://doi.org/10.5194/acp-15-10529-2015

TEDB. (2021). Transportation energy data Book table 3.02-3.04.

Thiruvengadam, A., Besch, M. C., Thiruvengadam, P., Pradhan, S., Carder, D., Kappanna, H., et al. (2015). Emission rates of regulated pollutants from current technology heavy-duty diesel and natural gas goods movement vehicles. *Environmental Science & Technology*, *49*(8), 5236–5244. https://doi.org/10.1021/acs.est.5b00943

Verstraeten, W. W., Neu, J. L., Williams, J. E., Bowman, K. W., Worden, J. R., & Boersma, K. F. (2015). Rapid increases in tropospheric ozone production and export from China. *Nature Geoscience*, *8*(9), 690–695. https://doi.org/10.1038/ngeo2493

Wang, Y., Ge, C., Castro Garcia, L., Jenerette, G. D., Oikawa, P. Y., & Wang, J. (2021). Improved modelling of soil NO_x emissions in a high temperature agricultural region: Role of background emissions on NO_2 trend over the US. *Environmental Research Letters*, *16*(8). https://doi.org/10.1088/1748-9326/ac16a3

Watanabe, S., Hajima, T., Sudo, K., Nagashima, T., Takemura, T., Okajima, H., et al. (2011). MIROC-ESM 2010: Model description and basic results of CMIP5-20c3m experiments. *Geoscientific Model Development*, *4*(4), 845–872. https://doi.org/10.5194/gmd-4-845-2011

Zara, M., Boersma, K. F., De Smedt, I., Richter, A., Peters, E., van Geffen, J. H. G. M., et al. (2018). Improved slant column density retrieval of nitrogen dioxide and formaldehyde for OMI and GOME-2A from QA4ECV: Intercomparison, uncertainty characterisation, and trends. *Atmospheric Measurement Techniques*, *11*(7), 4033–4058. https://doi.org/10.5194/amt-11-4033-2018

Zara, M., Boersma, K. F., Eskes, H., Denier van der Gon, H., Vilà-Guerau de Arellano, J., Krol, M., et al. (2021). Reductions in nitrogen oxides over The Netherlands between 2005 and 2018 observed from space and on the ground: Decreasing emissions and increasing O_3 indicate changing NO_x chemistry. *Atmospheric Environment: X*, *9*. 100104.

Zhang, R., Wang, Y., Smeltzer, C., Qu, H., Koshak, W., & Boersma, K. F. (2018). Comparing OMI-based and EPA AQS in situ NO_2 trends: Towards understanding surface NO_x emission changes. *Atmospheric Measurement Techniques*, *11*(7), 3955–3967. https://doi.org/10.5194/amt-11-3955-2018

Zhang, Y., Cooper, O. R., Gaudel, A., Nedelec, P., Ogino, S. Y., Thompson, A. M., & West, J. J. (2016). Tropospheric ozone change from 1980 to 2010 dominated by equatorward redistribution of emissions. *Nature Geoscience*, *9*(12), 875–879. https://doi.org/10.1038/ngeo2827

Zheng, B., Tong, D., Li, M., Liu, F., Hong, C., Geng, G., et al. (2018). Trends in China's anthropogenic emissions since 2010 as the consequence of clean air actions. *Atmospheric Chemistry and Physics*, *18*(19), 14095–14111. https://doi.org/10.5194/acp-18-14095-2018